Picosecond Spectrochronography

ARVI FREIBERG AND PEETER SAARI

Abstract—The general problem of extracting complete (amplitude and phase) information out of an optical signal is discussed. We have shown that the best one can do to determine all essential features of light pulses is to apply simultaneous temporal and spectral analysis to take spectrochronograms with the appropriate shape of the resolution cell on the ωt-plane. We use the term "spectrochronogram" instead of the much broader term "time-resolved spectrum" for a specific measurement result where the resolutions $\Delta\omega$ and Δt used are transform correlated. A novel subtractive mount of monochromators has been proposed to overcome the obstacles to experimental realization of uncertainty-principle-limited setups for high spectral resolution picosecond spectrochronography. For the examples of perylene and anthracene molecules, experimental spectrochronograms revealing temporal behavior of hot luminescence lines and, correspondingly, picosecond kinetics of intramolecular vibrational relaxation have been presented. Some further applications of picosecond spectrochronography have been discussed.

I. Introduction

With the development of single-mode lasers on the one hand, and of mode-locked lasers on the other, several concepts and methods have been introduced into optics which have already been well known in radiospectroscopy. Nevertheless, one should not forget the principal differences between these fields. There are no optical oscilloscopes that can display the waveform of a light signal in the way familiar from radioelectronics, and the only possibility to record the signal is square-law detection. Moreover, when considering spontaneous optical responses of a material system, rather than the strong coherent or stimulated ones, quantum stochasticity [1] is involved. The result is the loss of the phase information in the light detection process with well-known consequences—indistinguishability of T_1, T_2, and inhomogeneous broadenings of a spectral line on the one hand, or unobservability of frequency modulations in direct time-domain measurements (not to mention indirect correlation techniques, which, as is known to picosecond spectroscopists, do not provide sufficient data even on the pulse-amplitude envelope) on the other. Although under certain conditions essential characteristics of the signal (and, hence, of the excitation in a material system) can, after all, be reconstructed, an intriguing question arises—is there any general way to extract complete information out of a light-emission signal? The answer seems to be obvious: one should combine spectral and temporal resolutions. However, a problem of the physical nature of a time-dependent spectrum arises here. As has been shown in [2]-[6], a rigorous definition of such a quantity must consistently take into account the measurement process and, hence, the uncertainty relation $\Delta\omega \cdot \Delta t \simeq 1$ between extremal spectral and time resolutions. It should be pointed out that the measurement by an interrogative (probe) beam naturally obeys the same relation. If the product $\Delta\omega \cdot \Delta t$ approaches its transform-limited value, we propose a record of the quantity to be termed a spectrochronogram in order to draw a distinction between this specific case and a general case of a "time-resolved spectrum," measured under conditions where the time resolution is not limited by the spectrum, but rather in a trivial manner, by the rate of processes or electronics involved after the primary act of photon detection. The physical meaning of the spectrochronogram will be discussed in the next section. In Section III, we shall touch on some hardware problems and describe our picosecond spectrochronograph.

Theoretical discussions of several problems connected with spectrochronography can be found in review papers by Rebane, Hizhnyakov, and Schubert in [7], [8], and by Takagahara, Toyozawa, and Mukamel in [9]. However, the advantages of spectrochronography are, perhaps, most transparent in the case of population kinetics studies in a multilevel emitting system with close-level spacing. If the levels belong to vibrational substates of an excited electronic state in condensed matter, the emission is hot luminescence (HL) [10], the rise/decay behavior of different spectral parts of which gives a complete picture of vibrational energy relaxation in the excited system. A consistent treatment of HL requires other possible transient components (first of all, resonant Raman scattering) of the secondary light emission at resonance excitation to be involved. A corresponding conceptual framework along with the theory has been developed in our institute during the past decade. With reference to several review papers (e.g., [11]-[13]) for a more thorough introduction into the field, in Section IV we shall present, as the first example of spectrochronography applications, some experimental spectrochronograms revealing HL.

The temporal behavior of a material excitation need not always be depictable by a limited number of decay constants. One can come upon much more complicated and interesting patterns of time evolution and transformation of excitations, especially when studying low-temperature solids. Such a study requires an untangling of certain frequency modulations from the signal. So, here opens a proper field of exploiting spectrochronography as a demodulation procedure in optics. It is interesting to note that there is a far-reaching resemblance between the spectrochronograph scheme described in Section III and a phase discriminator—the radioelectronical device for the demodulation of FM signals. From this point of view, in Section V of this paper, we shall briefly discuss some further applications of picosecond spectrochronography.

Manuscript received August 9, 1982; revised January 17, 1983.

The authors are with the Institute of Physics, Estonian SSR Academy of Sciences, Tartu 202400, USSR.

0018-9197/83/0400-0622$01.00

II. What is a Spectrochronogram?

Obviously, if at the beginning, for simplicity, one does not consider stochastic emission of incoherent ensembles, then a complete representation of the emitted light pulse is an oscillogram of its waveform. However, in order to measure such an oscillogram, one needs equipment with a bandpass that far exceeds the carrier frequency. Since this is unfeasible at optical frequencies, the time-domain measurement gives a more-or-less smoothed profile of the light signal envelope, and the information about the phase, i.e., about the carrier frequency and its changes, is lost. If one tries to overcome this obstacle by passing over to the frequency domain, one is still not able to reconstruct the signal from the experimental data since in this case, the information about the relative phases of spectral components is lost in the light-detection process.

A promising way of mastering these difficulties is an application of both time and spectral resolutions, not by simply restricting oneself to comparing the spectrum and the temporal behavior of the emitted light intensity, but by making a comprehensive measurement of the time dependence of the spectrum. However, the term "instantaneous spectrum" is an intrinsically contradictory quantity, due to the complementarity between time and frequency representations.

A physically clear and distinct way of displaying the time dependence of light emission can be obtained by introducing a signal trajectory as a curve in the frequency-time-intensity ωtI-space. The projection of this curve onto the ωt-plane gives the time dependence of the instantaneous value of the carrier frequency $\omega(t) = \dot{\phi}(t)$ of the signal $ReE^{+}(t)$ ($E^{+} = A(t)\, e^{-i\phi(t)}$). (The feasibility of determining $\omega(t)$ experimentally for picosecond laser pulses was first considered in [14].) The projection of the trajectory onto the It-plane gives the time dependence of the amplitude envelope ($I(t) = |A(t)|^2$). In Fig. 1, a simple model situation is depicted to illustrate the essence of the matter. The trajectory introduced, for certain conditions of limited bandwidth, presents the same information as the oscillogram does, so the aim of an experiment should be to determine the shape of the trajectory as precisely as possible via a physically measurable time-dependent spectrum.

The problem of a rigorous definiton of the latter quantity is discussed in [2]-[6]. A physical time-dependent spectrum $I(\omega, t)$ can be defined through an instrument (tuned to ω) function $F_\omega(t)$

$$I(\omega, t) = \left| \int F_\omega(t - t') E^{+}(t')\, dt' \right|^2 \tag{1}$$

or, rewritten for a quantum-mechanical ensemble [4]

$$I(\omega, t) = \iint F_\omega^{*}(t - t') F_\omega(t - t' - \tau) G(r, t', \tau)\, dt'\, d\tau \tag{1a}$$

for which the emitted field at the point r is determined by the correlation function $G(r, t, \tau) = \langle E^{-}(r, t) E^{+}(r, t + \tau) \rangle$, E^{-} and E^{+} being the negative- and positive-frequency components of the electric field operator, respectively.

In the steady-state case, when G does not depend on t, $I(\omega, t)$ results in an expression of the spectrum convolution with the instrument bandpass function profile, which is familiar in spectroscopy. In the particular case of a spectrograph with normal slitwidth, as shown in [4], one can put $F_\omega(t) = T^{-1}[Y(t) - Y(t - T)] \exp(-i\omega t)$, where Y is the Heaviside unit step and ω is the spectrum frequency under examination. T equals the interval between the waves coming from the right and left edges of the grating, or the exposure time when time resolution is accomplished by a light shutter in front of the spectrograph (see Section III). Thus, it determines the integration interval of the field, i.e., the time resolution $\Delta t = T$, as well as the spectral resolution $\Delta\omega \simeq 2\pi/T$.

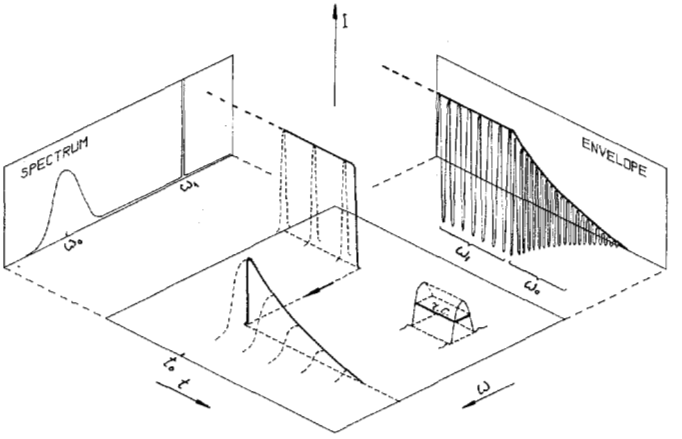

Fig. 1. Right-hand side: the wave emitted by a damped oscillator in case of a sinusoidal driving force. At $t = t_0$, the driving force is abruptly turned off and the forced vibration turns into free decaying vibration at the natural (resonance) frequency ω_0. Left-hand side: the spectrum of the wave. Foreground: the solid curve—the trajectory in the ωtI-space representing the temporal behavior of the amplitude and carrier frequency of the wave; dashed curves—intersections of an imaginable "instantaneous spectrum." The rectangle rc depicts a Gabor-type resolution cell of an area $\Delta\omega \cdot \Delta t = 2\pi$, which may be ascribed to a prism or grating spectrograph with the response duration Δt (and, correspondingly, sinc-function-shaped spectral response of FWHM = $\Delta\omega$).

So, the uncertainty $\Delta\omega \cdot \Delta t \simeq I$ is inherent to $I(\omega, t)$, and the latter can be imaged as a set of response intensities on a grid of "elementary instrument cells" in the ωt-plane. Due to the finite area of these Gabor-type cells, the surface of $I(\omega, t)$ resembles a quilted blanket, covering the ωt-plane with the trajectory curve above the plane, rather than a silk cloth hanging on the curve. Therefore, from a spectrochronogram, the trajectory can hardly be recognized (Fig. 2). In addition, the spectrochronogram exhibits some characteristic oscillations. The reason for the latter is interference effects in the course of convolution formation between the signal amplitude and oscillatory "fine structure" of the response at the resolution cell. Hence, the spectrochronogram is a result of an analysis of the temporal behavior of the frequency contents of light, when the instrumentation comes close to achieving the minimum uncertainty $\Delta\omega \cdot \Delta t$, and specific features of the intensity surface appear on the ωt-plane due to the correlations between its points. The slower and the more large-scale the trajectory changes are, the more directly they can be displayed by choosing an appropriate shape of the resolution cell to record the spectrochronogram (Fig. 3).

As for definitions, the term "time-resolved spectrum" should preferentially be used as the result of a measurement on a large ωt-scale, where the resolutions $\Delta\omega$ and Δt are not

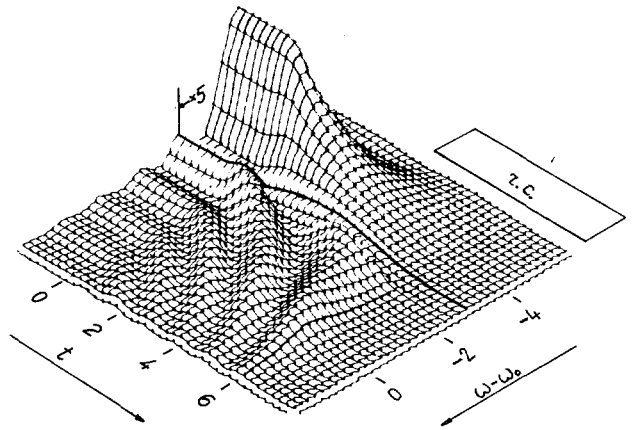

Fig. 2. Spectrochronogram, calculated for the model situation of Fig. 1. Right-hand side: the resolution cell corresponding to $\Delta t = 6$ is shown. The oscillator decay constant has been taken as a time unit, its reciprocal, as a unit for the emission frequency $\omega - \omega_0$. After the driving force of a frequency $\omega_1 = \omega_0 - 4$ is switched off at $t = 0$, one can observe a nonmonotonic behavior of the intensity around the emitter frequency, which transforms into an exponentially decaying Lorentzian-like band at $t = 6$, i.e., after the spectrograph has forgotten the carrier frequency jump.

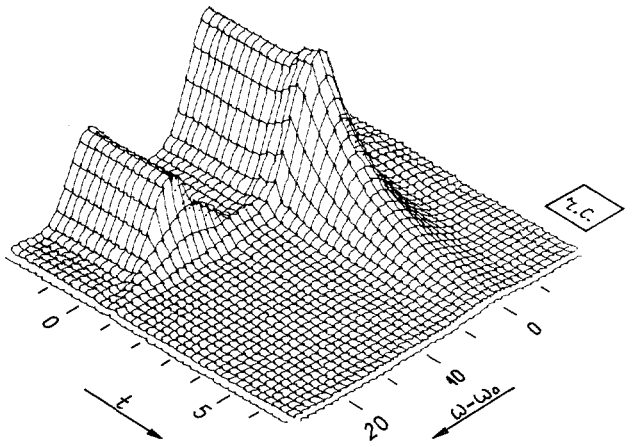

Fig. 3. Spectrochronogram calculated according to (1a) for the secondary light emission of an ensemble of two-level systems subjected to excitation by a long, but weak, rectangular laser pulse and, unlike the previous example, impact-type relaxation. As compared to Fig. 2, the excitation frequency detuning is much larger ($\omega_1 - \omega_0 = 16$) and of the opposite sign (to place the trajectory of forced vibrations, i.e., of scattered light in the forefront). After the driving field is switched off at $t = 0$, the scattering dies out within $\Delta t = 1$ (chosen equal to the reciprocal of FWHM of the absorption line), while the emission at the free-running frequency of the system (i.e., luminescence), after a little increase due to the excitation switchoff, decays exponentially with the depopulation rate of the upper level, which is taken equal to 0.6 (for details see [15]).

transform correlated, but are determined separately by the parts of the setup with $\Delta\omega\Delta t \gg I$. On the other hand, the term "dynamic spectrogram" introduced in [14] for representing carrier frequency changes in deterministic laser pulses should not, in our opinion, be extended to the quantity determined by expression (1a).

Let us note that in the case of a statistical ensemble of emitters, each particular realization of the trajectory loses meaning, and a distribution of trajectories should be considered, which in the general case is, in fact, conveyed by a spectrochronogram. It should be recalled that the quantum-mechanical picture of photon spontaneous emission involves an ensemble (of experiments) even in the case of one emitter. Finally, one need not analyze spectrochronograms on the basis of trajectories only. From $I(\omega, t)$, one can deduce physically less transparent, but unambiguously determined quantities, such as the correlation function $G(t, \tau)$ and/or a time-dependent power spectrum, which is Fourier correlated to the former [6].

To conclude, in the optical domain, where a measurement inevitably provides only partial information on a light waveform, the best we can do to determine all essential features of nonstationary light emission is to take spectrochronograms with appropriate shapes of the resolution cell.

III. Experimental

From the experimentalist's point of view, the problem is reduced to creating an apparatus which is able to resolve, with a sufficient sensitivity, the area in the ωt-plane approaching as near as possible the minimum value $\Delta\omega\Delta t \simeq 1$. For this, the following two general types of setups exist: 1) a shutter placed in front of a spectrometer and triggered by a picosecond laser pulse via some nonlinear phenomenon; and 2) a spectrometer with a sufficiently fast photodetector behind it. In either case, the possibility of a simultaneous following of the evolution of many spectral components in time requires a recording with multichannel optical detectors. Analyzing the possible advantages and drawbacks of these two principal setups, one reaches the conclusion that, at the current technical level, mode-locked CW lasers with extremely stable transform-limited pulses and modern high-speed optical data recording by synchroscan streak cameras, the latter setups guarantee higher sensitivity, dynamic range, stability, flexibility, and even higher temporal resolution. This is not the case with the signal up-conversion setup, where the temporal resolution can be determined mainly by laser pulse duration. On the other hand, the former type of setups are generally simpler and less expensive.

Owing to a fundamental property of a spectral filter, the spectrometer not only determines the spectral resolution, but it also introduces temporal dispersion which, as a rule, considerably exceeds the value of Δt determined by spectral resolution through the uncertainty relation. Here, the reasons, similar to those discussed in the previous sections, are associated with the phase factor; in a real spectrometer, residual aberrations and geometrical imperfections cause substantial phase modulations in the pulse response function. Since the intensity envelope of the response is not sensitive to the modulation of its carrier frequency, while its spectral content is, the measurable pulse response should follow certain "ideal" (rectangular, as is the case in Section II) profiles, for the given spectrometer, while the profile of the frequency transmission band is affected and broadened by "nonideality." This seems to be a general rule for any spectral instrument, and the only obvious way to compensate for the nonideality is a substantial aperture restriction. In [16], [17], we treated the problem quantitatively and showed the possibility of the pulse response narrowing up to its transform-limited value in a substractive dispersion high-luminosity double monochromator at a supernormal width of the intermediate slit. Here, it is worth recalling that in the

substractive dispersion monochromator, the same dispersion elements in both parts of the monochromator are connected on substractive mode to give zero dispersion at the exit slit. The spectral resolution of such a monochromator is determined by the dispersion in the plane of the intermediate slit and by its geometrical width. The price one has to pay for that simple solution to the excess temporal broadening problem in a spectral apparatus is losing the possibility of carrying out the experiments with simultaneous recording of many spectral components—the spectral axes to be scanned point-by-point.

Experimental problems may still arise, which obviate simultaneous resolving of the whole spectrum in time. This can be coped with by a polychromator with an aperture restricted to a required extent (Fig. 4). The aperture restriction holds only in one direction, which, in a grating instrument, is perpendicular to the grooves of the grating. So, in this case, the result is reached at the expense of the signal-to-noise ratio, which in picosecond experiments is critical anyway. It should be noted that as long as the achievement of the minimum value of $\Delta\omega\Delta t \simeq 1$ is hindered by the optical imperfection of the grating, there is, in principle, a possibility of improving the situation by a proper optimization of this unit. But it should be stressed that decreasing $\Delta\omega \cdot \Delta t$ cannot be accomplished simply by using a coarser grating. For given aberrations and luminosity of collimating optics, the coarser the grating, the shorter the time response. This occurs at the expense of $\Delta\omega$; hence, the product $\Delta\omega \cdot \Delta t$ remains too large. A clever way to restore the effective aperture of the grating under circumstances close to spectrochronography has been proposed in [14], but this method is not convenient for use over a wide spectral range.

The picosecond spectrochronograph used in this work (Fig. 5) is based on a combination of a spectra physics mode-locked CW oxazine I dye laser, synchronously pumped at 82 MHz by a krypton-ion laser, a spectrometer, and a streak camera. For data recording and processing, an EC IOIO computer-controlled B&M Spektronik OSA 500 optical multichannel analyzer with an SIT vidicon is used.

For spectroscopic applications with temporal resolution, the most essential system parameters are the spectral tuning range, time and spectral resolutions, detection threshold, and dynamic range.

The tuning range of our dye laser with a two-plate birefringent filter as the tuning element is 685–805 nm. The real time scanning-autocorrelator-measured 3 ps nearly transform-limited pulses have peak power within the range of 100–1000 W. Using an $LiIO_3$ angle-tuned frequency doubler, excitation in the 345–400 nm UV region is achieved. The second harmonic generation efficiency reaches 1 percent.

As a spectrally resolving instrument, a substractive dispersion mount of two high-luminosity single-grating monochromators MDR-2 is used. The dispersion of the MDR-2 with replaceable 1200 and 600 groove/mm gratings is 2 and 4 nm/mm, respectively. The temporal response function of the monochromator is obtained by means of 3 ps dye laser pulses at ~750 nm, and a streak camera setup "Agat-SF" in single-shot operation with a temporal resolution (FWHM) of 8 ps. The smallest intermediate slit spectral width at which the response was detectable

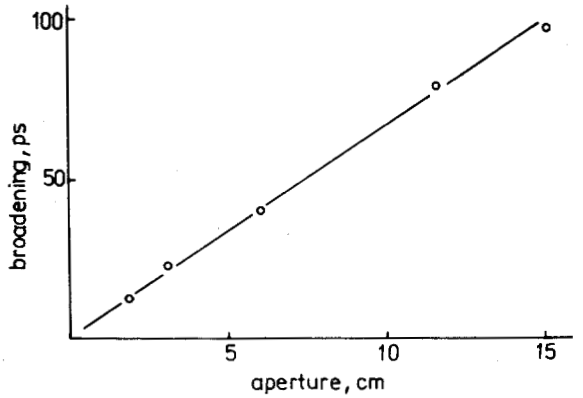

Fig. 4. The dependence of the single-grating 40 cm focal-length high-luminosity (1:2,5) monochromator MDR-2 response FWHM on the width of the working aperture on a 600 groove/mm grating, as tested by 3 ps dye laser pulses at 750 nm.

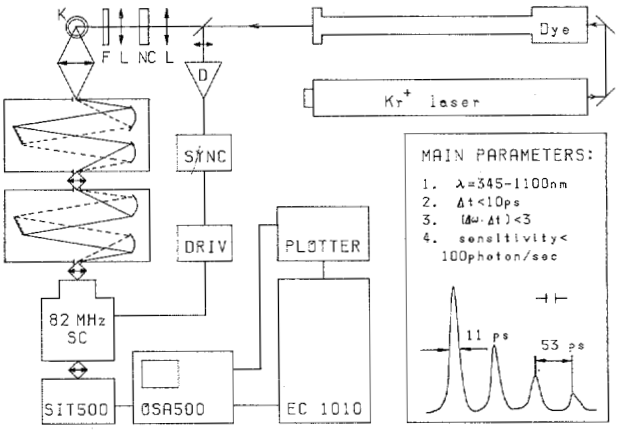

Fig. 5. Picosecond spectrochronograph for studying time-resolved emission spectra with uncertainty-principle-limited resolutions. *L*: lens, *NC*: nonlinear crystal for second harmonic generation, *F*: filter, *K*: cryostat, *SC*: synchroscan streak camera, *D*: photodiode, *SYNC*: synchronization unit, *DRIV*: streak camera driver. Right-hand side: the main parameters of the spectrochronograph and the test picture showing fine temporal resolution are displayed. FWHM of streak camera response in the statical (without streaking) mode is also indicated.

was 7 cm^{-1}. In this case, as shown in Fig. 6, no remarkable pulse broadening occurred. At the same time, an additive dispersion double monochromator with the same spectral slitwidth showed an extremely poor temporal response. A comparison should also be made with the temporal resolution of a single unit of MDR-2 with a filled aperture in Fig. 4.

The data recording system is based on a streak camera with UMI-93M or PV-001A/PMU-1 image converter tubes having a 1–2 ps temporal resolution. Instead of commonly used pulsed deflection, continuous streaking in synchronism with the picosecond CW dye laser operation [18], [19] is used. Maximum sweep rate at the center of the streak camera output screen is 3 cm/ns. For the synchronization of deflection and laser pulses, the following two methods [20] were used: 1) the sinusoidal RF signal of the acoustooptic mode-locked driver is doubled to 82 MHz, amplified up to 3 kV, and then used as deflection voltage. At the expense of time-consuming laser optimization and 30–50 percent loss in the average power, this method gives, at best, a temporal FWHM = 30 ps; and 2) the amplified out-

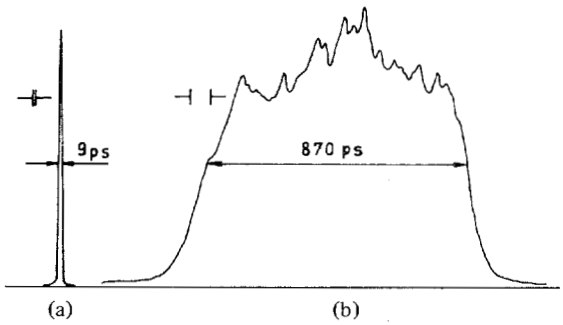

Fig. 6. Streak camera-measured temporal response of double monochromator with completely filled aperture and with slits giving ~7 cm^{-1} spectral resolution. (a) Subtractive dispersion monochromator compiled from two monochromators MDR-2 (600 grooves/mm, 1:2.5, $F = 40$ cm, 4 nm/mm). (b) DFS-24—a common Raman-quality spectrometer (1200 grooves/mm, 1:5.3, $F = 82.2$ cm, 0.5 nm/mm). FWHM's of streak camera responses are indicated.

put voltage of a signal generator, working with a recurrence frequency close to that of the laser, is used for deflection. This frequency is locked to the laser by a fast photodiode. By this method, a very stable, approximately 10 ps, spectrochronograph temporal response (see Fig. 5) was achieved. The quasi-steady image on the streak camera output screen is recorded by means of an SIT vidicon and fed (with the speed of 500 channels/8 s) into the computer EC IOIO for further treatment. In the present case, the computer treatment consists of data correction for changes in sensitivity as a function of the position (time) in the streak camera and in one- or two-exponential least-squares fitting of experimental curves, taking into account the temporal response function of the spectrochronograph.

The sensitivity of the spectrochronograph was estimated by comparing it with that of an FEU-106 photomultiplier working in the single-photon counting mode; the spectrochronograph unit signal level corresponds to the 50–100 photons on the streak camera photocathode (multihalide cathode). The linear dynamic range was measured to be $>10^3$, and was found to be limited on the upper end by the A/D converter of the OSA 500, and on the lower end by the noise of the streak camera [21].

The samples—frozen solutions of perylene in n-heptane (with saturated concentration of $\sim 10^{-4}$ M/l), and anthracene in fluorene ($<10^{-5}$ M/l)—were placed into a liquid He cryostat. Tightly focused frequency-doubled excitation pulses from a dye laser with an average power density of 6–30 W/cm^2 were used. The spontaneous emission at ~90° to the excitation direction was gathered with the aid of high-luminosity optics and focused onto the MDR-2 input slit. The temporally equidistant train of pulses, obtained by the laser beam passage through the Fabry-Perot interferometer, served for the calibration of the spectrochronograph time axis (see Fig. 5).

IV. Vibrational Relaxation Kinetics in the Excited S_1 Electronic State of Some Organic Molecular Systems

Here, we present and discuss the results of the first direct observation of the picosecond range temporal behavior of vibronic lines in the luminescence spectrum of the paraffine-

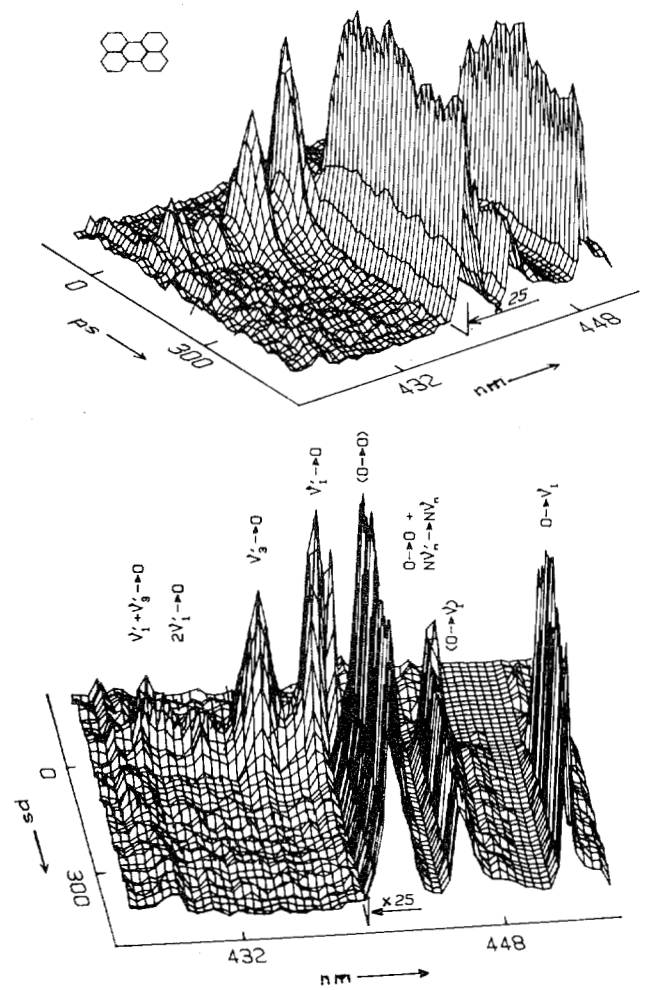

Fig. 7. Two views of the spectrochronogram of the fluorescence of perylene molecules (near the 0–0 transition region) in the n-heptane matrix at 4.2 K. The spectral width of the intermediate slit is 31 cm^{-1}. At $t = 0$ an excitation by frequency-doubled 3 ps long and 5 cm^{-1} spectrally wide laser pulses at $\lambda = 393.8$ nm populate a selected high-lying intramolecular vibrational level of S_1 manifold. For other details see the text.

matrix-isolated perylene molecules (see also [22], [23]) and anthracene molecules in the fluorene crystal. From the spectrochronograms obtained, vibrational lifetimes of the molecular system levels in the S_1 state were derived.

The three-dimensional spectrochronograms of the resonance secondary emission of perylene molecules in the n-heptane matrix at 4.2 K under excitation, which is ~2880 cm^{-1} higher than the 0-0 transition energy, is displayed in Fig. 7. On the right-hand side of the change of the intensity scale, four slowly decaying (with 5–6 ns time constant) ordinary (i.e., vibrationally relaxed) luminescence (OL) lines are seen. On the left, one can observe four short-lived HL lines arising, due to the radiative transitions from the excited levels of two lowest totally symmetric vibrational modes of the perylene molecule populated in the course of the excitation energy relaxation process in the S_1 state. The transitions are assigned by indicating the initial and final vibrational levels in the excited and ground electronic states, respectively.

In the Shpolskij systems, there ordinarily exist some types of inhomogeneous centers having, on the whole, similar spectra,

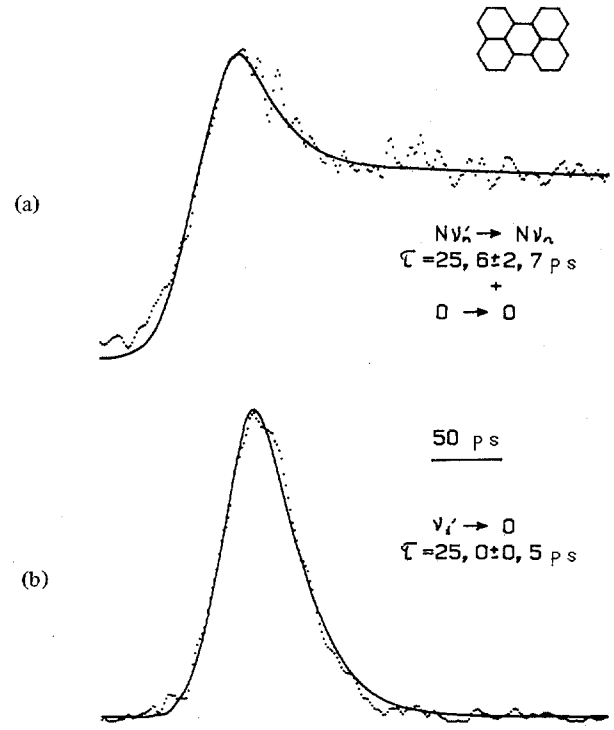

Fig. 8. The time axis cuts of the spectrochronogram shown in Fig. 7 at (a) $\lambda = 446$ nm and (b) $\lambda = 438$ nm. Solid lines represent the least-squares fit of the dotted experimental curves. The spectrochronograph temporal response function has FWHM = 40 ps. The given lifetimes are averaged over a number of measurements.

but different transition frequencies. One has to also note the essential advantages of measuring the broad inhomogeneous spectra with time resolution in order to distinguish the spectal components of different origins and to interpret the spectra properly. In the present case, one sees two distinct series of OL lines which correspond to two types of perylene impurity centers: "red" and "blue" (marked in Fig. 7 with brackets). All HL lines belong to the "red" centers, which have considerably higher density [the 0-0 line of these centers is suppressed by reabsorption (for details see [23])].

In Fig. 8, the time axis cuts of the spectrochronogram at the 0-0 and $\nu_1' \rightarrow 0$ transition wavelengths are given. If the shape of the latter is quite well-approximated with the convolution of the spectrochronograph response function and the one-exponential decay, the shape of the former is much more complicated. This is due to the overlapping of rapidly decaying $N\nu_n' \rightarrow N\nu_n$-type hot transitions to 0-0 transition (the perylene intramolecular vibrational quanta differ only slightly in S_0 and S_1 electronic states).

The decay time of the S_1 state vibrational levels obtained by the one-exponential least-squares fit of experimental curves are gathered in Table I. For comparison, in the last column, the decay times estimated from the steady-state HL spectrum [24] are also shown.

Analogous measurements were performed in mixed crystal-anthracene in fluorene. An essential advantage of this system is that with our dye laser, we are able to tune the excitation almost over the whole $S_0 \rightarrow S_1$ absorption band and thus, to investigate the peculiarities of the relaxation of different amounts of excess vibrational energy.

TABLE I
LIFETIMES τ (ps) FOR THE LOWEST VIBRONIC LEVELS OF A PERYLENE MOLECULE IN n-HEPTANE AT 4.2 K

Vibrational energy in S_1 state (cm^{-1})	Assignment to vibrational modes	τ (this work)	τ ([24])
1580	ν_9'		10±3
1380	ν_8'		5±2
1300	ν_7'		14±3
900	$\nu_1' + \nu_3'$	15.7±2.5	
710	$2\nu_1'$	21.0±1.4	
550	ν_3'	26.0±2.2	
360	ν_1'	25.0±0.5	35±5

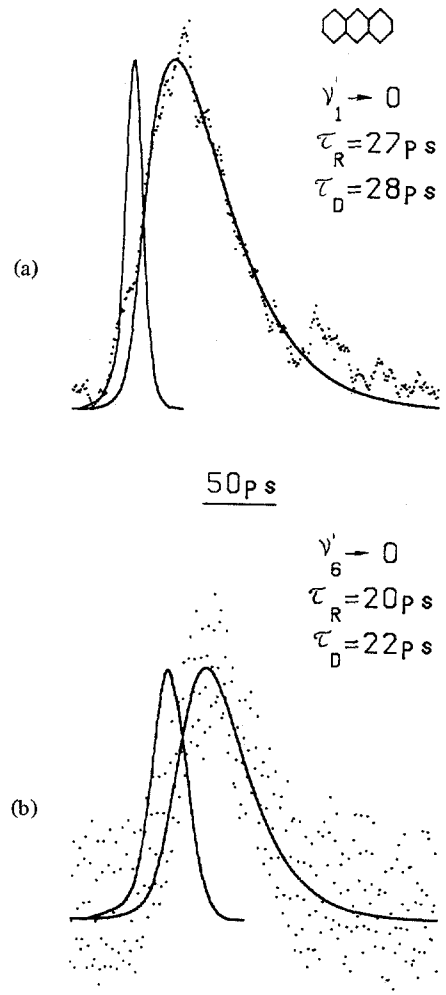

Fig. 9. The time axis cuts of the anthracene fluorescence spectrochronogram: (a) at 380 nm (excitation at 373.4 nm or 0-0 + 2 × 400 cm^{-1}); (b) at 369 nm (363.8 nm - 0-0 + 1500 cm^{-1}). The spectrochronograph response functions, indicating the zero time point, are also shown. τ_R and τ_D denote the rise and decay times, respectively. Other details are the same as in Figs. 7 and 8.

In this work, two excitation frequencies were used, corresponding to the excitation up to the $2 \times \nu_1' \simeq 800$ cm^{-1} and $\nu_7' \simeq 1500$ cm^{-1} vibrational Franck-Condon levels in the S_1 state of anthracene. As expected, in the first case [Fig. 9(a)], only one HL line ($\nu_1' \rightarrow 0$) is detected. (Strictly speaking, the lines of type $N\nu_n \rightarrow (N-1)\nu_n$ overlap with lines $\nu_n' \rightarrow 0$, but

TABLE II
TIME CONSTANTS τ_R AND τ_D (ps) FOR THE LOWEST VIBRONIC LEVELS OF AN ANTHRACENE MOLECULE IN FLUORENE AT 4.2 K. EXPERIMENTAL ERROR ±15 PERCENT

Vibrational energy in S_1 state (cm^{-1})	Assignment to vibrational modes	τ_R	τ_D	τ ([24])
1500	ν_7'			6±1
1400	ν_6'	20	22	3.5±1.5
400	ν_1'	25	28	

in certain cases their contribution is small.) In the second case (for steady-state spectra at this excitation see [24]), one additional HL line ($\nu_6' \rightarrow 0$) is seen [Fig. 9(b)]. All relaxation constants derived are gathered in Table II (constants for $\nu_1' \rightarrow 0$ transition under different excitation conditions coincide within experimental error).

It is clear from these results that the energy relaxation processes in the two systems under study are quite different. In the case of perylene, the HL level population processes are very fast, which is expressed in the exciting-pulse-limited rise time of HL lines (Fig. 8). On the contrary, the HL lines in the system with anthracene are growing slowly. As can be seen from Table II, the $\nu_1' \rightarrow 0$ HL line rise time coincides within a 15 percent experimental error with the $\nu_6' \rightarrow 0$ line decay time. Probably, this is due to the excitation conditions used. It seems that under low-excess vibrational excitation energy, the most important relaxation pathways go essentially through Franck-Condon levels, which in the cases under study have rather long decay times and give rise to the bottleneck effect for the rise times of the HL lines. This effect should also be expressed in the retardation of the OL rise time, but in practice it is hardly noticeable on the background of the slow OL rise. Yet the data for the anthracene vibrational relaxation kinetics have to be specified, due to a rather low signal and poor signal-to-noise ratio.

The energy relaxation times measured are surprisingly long if one considers the relative complexity of the molecules and the existence of the phonon bath of the matrix. These interesting aspects, as well as some other features of vibrational energy relaxation, including the microscopic investigation of the relaxation mechanisms in complex and semicomplex molecules, need further study.

Finally, comparing measured relaxation constants with those estimated from the steady-state HL spectrum, one notices quite large discrepancies, especially in the case of anthracene. This is not surprising, when keeping in mind the difficulties one has to overcome in deriving the HL line intensities from inhomogeneous spectra and the roughness of the approximations used.

V. FURTHER APPLICATIONS

Let us now consider a system (e.g., a molecule) in which a particular vibrational mode is excited so highly after the laser pulse (it can occur via a one-photon process in the case of a strong electron-phonon coupling) that, due to the high phonon number, the vibration follows a classical pattern. As the frequency of the emitted light is modulated by the vibration through electron-phonon coupling, the emission trajectory should be a lying sinusoid on the ωt-plane, whose frequency-sweep amplitude decreases with time in accordance with the relaxation of the vibration, and which subsides on the plane in accordance with electron-oscillator damping. Thus, in the given case, which is typical for color centers in solids, spectrochronography enables us to reveal information on vibration (or vibrations), which manifests itself in conventional spectra as a wide structureless band. Model calculations of spectrochronograms for color centers with strong electron-phonon coupling have been carried out in [5].

Let us stress that the description of the relaxation of an excitation by a well-known picture of the constants T_1 and T_2, for determining which of a number of sophisticated techniques have been developed, is possible only in impact approximation, and becomes invalid at low temperatures. Such a non-Markoffian type of relaxation should be described through the characterizing of the fluctuations acting on a relevant dynamical system. As could be already seen on the simplest example of polarizability with a frequency denominator $(\omega_0^2 - \omega_1^2 - i\omega_1\gamma)^{-1}$, the fluctuations of the resonance frequency ω_0 affect both real and imaginary parts of the quantity. Thus, in order to investigate the fluctuations, one needs to untangle AM and FM in the optical response, which is again a proper task for spectrochronography. It is even more prospective in the study of the FM, caused by AM excitation, i.e., for a time-resolved study of strong-field effects (see theory in [25]).

In case the shape of the resolution cell is appropriately fitted to the field under study, the width of the spectrochronogram in the ω direction may turn out to be less than the natural one. In the case of pure lifetime broadening, if one chooses an exponentially decaying response function with the time constant equal to the lifetime, the spectral line is asymtotically (as $t \rightarrow \infty$) δ-shaped (see theory in [26], [27]), thus allowing a spectroscopy with a subnatural resolution. The physical reason for the narrowing effect is that the decaying light wave is normalized into a constant amplitude one in this specially fitted instrument and, therefore, it is processed the same way that a monochromatic wave would be processed in an ideal Fourier-transformer during the time interval t.

As to other scientific and technological applications, we have no possibility of discussing here such obvious ones as monitoring the performance of mode lockers, pulse shapers, and other high-speed devices, as well as some less-obvious ones, as used in investigations of photobiology [28], chemical reaction kinetics, explosion, plasma physics, and other fields of physical, chemical, and biological research, which all use one or another specific quality of the spectrochronograph. To close this section, we confine ourselves to presenting only one example demonstrating how the spectrochronograph described in Section III can easily be applied to solving certain problems (included technological) belonging to rather different fields of activity. In Fig. 10, a simultaneously temporally and spatially resolved GaAlAs heterojunction laser generation [29] is shown. In this case, the time axis is directed perpendicular to the exit slit of the spectrometer and the position is along the slit. Note the micrometer-range line dimension unit. High-obtainable

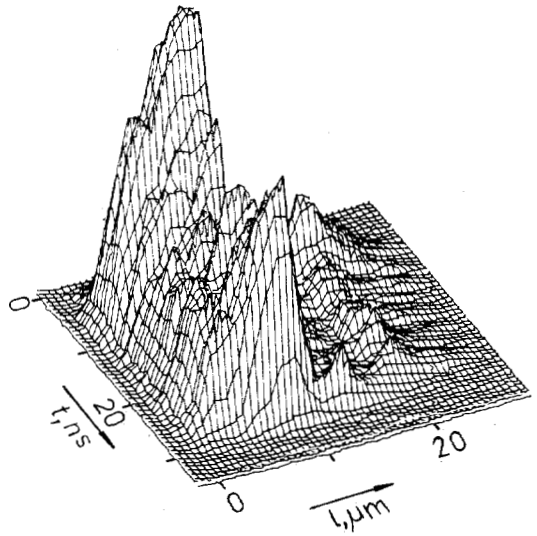

Fig. 10. Three-dimensional (time-position-intensity) representation of GaAlAs heterojunction laser generation enabling one to follow with high precision the generation picture both in time and in space.

spatial resolution opens new perspectives, e.g., in studying the spatial energy transfer processes in the pico-nanosecond range.

VI. Conclusions

We have demonstrated that on the current technical level of picosecond devices, not only is direct recording of the intensity decay curve for a reemission of a picosecond pulse absorbed in a material system feasible, but so is simultaneous high-resolution spectral analysis of the emitted light. Resulting spectrochronograms provide the maximum information on light pulse waveform achievable in optics. As predicted by theoretical studies and proven by first experiments, spectrochronography as such has the potential to become a productive technique for the investigation of transient light-emitting excitations in matter.

Acknowledgment

The authors are sincerely grateful to K. K. Rebane for support and numerous valuable discussions, as well as to J. Aaviksoo, A. Anijalg, T. Tamm, and K. Timpmann for their contributions to common experiments and the development of the method.

References

[1] R. J. Glauber, "The quantum theory of optical coherence," *Phys. Rev.*, vol. 130, pp. 2529–2539, 1963.

[2] J. H. Eberly and K. Wodkiewicz, "The time-dependent physical spectrum of light," *J. Opt. Soc. Amer.*, vol. 67, pp. 1252–1261, 1977.

[3] E. Courtens and A. Szöke, "Time and spectral resolution in resonance scattering and resonance fluorescence," *Phys. Rev. A*, vol. 15, pp. 1588–1603, 1977.

[4] P. M. Saari, "On the problem of observability in the theory of transient emission spectra," *ENSV TA Toimetised, Füüs. Matem.*, vol. 27, pp. 109–111, 1978.

[5] V. V. Hizhnyakov and I. K. Rebane, "Time dependent spectra of resonancce secondary emission," *Zh. Eksp. Teor. Fiz.* (in Russian), vol. 74, pp. 885–896, 1978.

[6] H.-E. Ponath and M. Schubert, "The time-space-dependent power spectrum for the description of nonstationary and inhomogeneous electromagnetic fields," *Ann. Phys. (Leipzig)*, vol. 37, pp. 109–120, 1980.

[7] "Ultrafast relaxation and secondary emission," in *Proc. Int. Symp. Ultrafast Phenomena in Spectrosc.*, ESSR Acad. Sci., Tallinn, Sept. 27–Oct. 1, 1978.

[8] "Ultrafast phenomena in spectroscopy," in *Proc. 2nd Int. Symp.*, Reinhardsbrunn, G.D.R. Acad. der Wissenschaften der DDR, Jena, Germany, Oct. 30–Nov. 5, 1980.

[9] "Relaxation of elementary excitations," in *Proc. Taniguchi Int. Symp.*, Susono-shi, Japan, Oct. 12–16, 1979, R. Kubo and E. Hanamura, Eds. Berlin: Springer-Verlag, 1980.

[10] P. M. Saari and K. Rebane, "Hot luminescence lines in the secondary radiation spectrum of KCL-NO_2^- and KBr-NO_2^- crystals," *Solid State Commun.*, vol. 7, pp. 887–890, 1969.

[11] K. K. Rebane, I. J. Tehver, and V. V. Hizhnyakov, "On the theory of resonant secondary radiation: Scattering, luminescence, and hot luminescence," in "Theory of light scattering in condensed matter," in *Proc. 1st Joint USA-USSR Symp.* New York: Plenum, 1976, pp. 393–406.

[12] K. Rebane and P. Saari, "Hot luminescence and relaxation processes in resonant secondary emission of solid matter," *J. Luminescence*, vol. 16, pp. 223–243, 1978.

[13] K. Rebane, "Resonant secondary emission by impurities in crystals," in *Light Scattering in Solids, Proc. 2nd USA-USSR Symp. on Light Scattering in Condensed Matter*, New York, 1979, J. L. Birman, H. Z. Cummins, and K. K. Rebane, Eds. New York: Plenum, 1979, pp. 257–267.

[14] E. B. Treacy, "Measurement and interpretation of dynamic spectrograms of picosecond light pulses," *J. Appl. Phys.*, vol. 42, pp. 3848–3858, 1971.

[15] P. M. Saari, "On the distinction between resonant scattering and hot luminescence, application of theory to experiment," in "Light scattering in solids," in *Proc. 2nd USA-USSR Symp. on Light Scattering in Condensed Matter*, New York, 1979, J. L. Birman, H. Z. Cummins, and K. K. Rebane, Eds. New York: Plenum, 1979, pp. 315–330.

[16] P. M. Saari, J. Aaviksoo, A. M. Freiberg, and K. E. Timpmann, "Elimination of excess pulse broadening at high spectral resolution of picosecond duration light emission," *Opt. Commun.*, vol. 39, pp. 94–98, 1981.

[17] —, "Elimination of excess pulse broadening at high spectral resolution picosecond light pulses," in *Proc. Int. Conf. on Lasers '81*, New Orleans, LA, Dec. 14–18, to be published.

[18] M. C. Adams, W. Sibbett, and D. J. Bradley, "Linear electron-optical chronoscopy at a repetition rate of 140 MHz," *Opt. Commun.*, vol. 26, pp. 273–276, 1978.

[19] A. M. Freiberg, A. Raidaru, A. O. Anijalg, K. E. Timpmann, P. Kukk, and P. M. Saari, "Streak camera operating in synchronism with a picosecond laser for real-time optical process measurement," *ENSV TA Toimetised. Füüs. Matem.* (in Russian), vol. 29, pp. 187–194, 1980.

[20] A. O. Anijalg, K. E. Timpmann, and A. M. Freiberg, "A real time spectrochronograph with time resolution better than 10 ps," *Pis'ma J. Techn. Phys.* (in Russian), to be published.

[21] A. O. Anijalg, A. M. Freiberg, R. Kaarli, P. Kukk, P. Saari, and K. E. Timpmann, "Investigation of ultrafast processes with the help of a continuously-operating streak camera," in *Proc. Int. Symp. "Ultrafast Phenomena in Spectrosc.,"* ESSR Acad. Sci., Tallinn, pp. 95–99, Sept. 27–Oct. 1, 1978.

[22] J. Aaviksoo, A. O. Anijalg, A. M. Freiberg, M. Lepik, P. M. Saari, T. B. Tamm, and K. E. Timpmann, "Direct picosecond resolving of hot luminescence spectrum," in *Proc. 3rd Topical Meet. on Picosecond Phenomena*, Garmisch-Partenkirchen, Germany, June 16–18, 1982, to be published.

[23] A. O. Anijalg, P. M. Saari, T. B. Tamm, K. E. Timpmann, and A. M. Freiberg, "Spectrochronography of hot luminescence as the method for the study of picosecond relaxation in molecular systems," *Kvantovaya Elektronika* (in Russian), vol. 9, pp. 2449–2454, 1982.

[24] T. B. Tamm and P. M. Saari, "Hot luminescence study of the intramolecular thermal bath of aromatics," *Chem. Phys.*, vol. 40, pp. 311–319, 1979.

[25] J. H. Eberly, C. V. Kunasz, and K. Wodkiewicz, "Time-dependent spectrum of resonance fluorescence," *J. Phys. B: Atom. Molec. Phys.*, vol. 13, pp. 217–239, 1980.

[26] I. K. Rebane, A. L. Tuul, and V. V. Hizhnyakov, "The time dependent quasiline spectra of resonant secondary emission," *Sov. Phys. JETP*, vol. 50, pp. 655–665, 1979.

[27] I. Rebane and V. Hizhnyakov, "On the theory of the measure-

ment of the time dependent spectra," *ENSV TA Toimetised, Füüs. Matem.* (in Russian), vol. 30, pp. 1–8, 1981.
[28] A. M. Freiberg, K. E. Timpmann, R. Tamkivi, and R. Avarmaa, "Investigation of picosecond fluorescence kinetics of chloroplasts fragments by synchronously-pumped dye laser and spectrochronograph," *ENSV TA Toimetised, Füüs. Matem.* (in Russian), vol. 31, pp. 200–207, 1982.
[29] I. Rammo, V. Vabson, and J. Haller, "The dependence of GaAs-GaAlAs heterojunction laser axial mode wavelength separation on cavity parameters," *ENSV TA Toimetised, Füüs. Matem.* (in Russian), vol. 30, pp. 22–28, 1981.

Arvi Freiburg was born in Kuremäe, Estonian S.S.R., U.S.S.R., in 1948. He graduated from The Tallinn Technical University and received the Candidate of Sciences degree in solid state physics in 1976 from the Institute of Physics, the Estonian Academy of Sciences, Tartu, of U.S.S.R. His thesis research concerned the electron-phonon interaction in the spectra of small molecular ions in crystals at low temperatures.

In 1980 he became Senior Research Associate at the Institute of Physics, the Estonian Academy of Sciences. His research interests include picosecond and nonlinear spectroscopy of condensed media and the application of contemporary experimental facilities including single-shot and synchroscan streak cameras. He is the author and coauthor of about 50 scientific papers.

Peeter Saari was born in Tallinn, Estonian, S.S.R., U.S.S.R., in 1945. He graduated from the Tartu State University, Tartu, U.S.S.R., in 1968. He received the Candidate of Sciences and the Doctor of Sciences degrees from the Institute of Physics, Estonian Academy of Sciences, Tartu, U.S.S.R., in 1972 and 1980, respectively.

He is presently the Director of the Institute of Physics, Estonian Academy of Sciences. His research interests include secondary light emission and ultrashort relaxation processes in molecules and impurity centers.

A Semiconductor Detector for Measuring Ultraweak Fluorescence Decays with 70 ps FWHM Resolution

SERGIO COVA, SENIOR MEMBER, IEEE, ANTONIO LONGONI, ALESSANDRA ANDREONI, AND RINALDO CUBEDDU

***Abstract*—The performance of a new single-photon avalanche photodiode particularly suitable for the detection of fast and ultraweak light pulses is described. The advantages of this device over other available detectors are discussed. The electronic circuitry developed allows the measurement of fluorescence decays with a time resolution of 70 ps FWHM (full-width at half-maximum) and a data acquisition rate of up to 50 kHz.**

I. INTRODUCTION

THE development of laser techniques for generating ultrashort light pulses at wavelengths from UV to IR has stimulated studies of ultrashort fluorescence phenomena in various fields, particularly in photochemistry and molecular biology. The difficulty of obtaining very short time resolution in measurements of fluorescence decay times is often increased by the low intensity of the light to be detected. The intensity level has to be evaluated with reference to the number N_{DR} of detected photons per resolving time T_R of the measurement. In order to obtain measurements having a high signal-to-noise ratio (S/N) with moderate or low N_{DR}, say with $N_{DR} < 10^4$, the measurement apparatus, besides having a short T_R, must: 1) have *averaging* capability, that is, it must accumulate the data obtained from many repetitions of the fluorescence pulse so that fluctuations due to the radiation statistics can be averaged out; 2) employ *photodetectors with high internal amplification* A_D, that is, transduction systems where one detected photon is transduced into a high number A_D of electrical conduction carriers (free electrons or electron-hole pairs). This requirement arises because of the electrical noise in the circuits of the measurement apparatus. In fact, in order to avoid degradation of the information carried, the electrical signal should be much higher than this noise, so that the lower the N_{DR}, the higher the required A_D.

The shortest resolving times among electronic methods, a few picoseconds, are provided by streak cameras. Some preamplification is provided in such apparatus by the accelerating voltage, and further amplification may be provided by the

Manuscript received August 4, 1982.

S. Cova and A. Longoni are with the Istituto di Fisica del Politecnico, Milano, Italy.

A. Andreoni and R. Cubeddu are with the Centro di Elettronica Quantistica e Strumentazione Elettronica del CNR, Milano, Italy.

0018-9197/83/0400-0630$01.00